Advanced Journal of Chemistry-Section A

Journal homepage: www.ajchem-a.com

Original Research Article

Phytosynthesis, Characterization and Antimicrobial Studies of Silver Nanoparticles Using Aqueous Extracts of *Olax Subscorpioidea*

Ochui Isaac Ashindortiang[1], Chinyere Ayi Anyama[2], Ayi Anyama Ayi[2,*]

[1] *Department of Chemistry, Faculty of Science, Cross River University of Technology, Calabar, Nigeria*

[2] *Inorganic Materials Research Laboratory, Department of Pure and Applied Chemistry, Faculty of Physical Sciences, University of Calabar, P.M.B. 1115, Calabar, Nigeria*

ARTICLE INFO

Article history

Submitted: 30 March 2022
Revised: 25 April 2022
Accepted: 02 May 2022
Available online: 03 May 2022
Manuscript ID: AJCA-2203-1307
Checked for Plagiarism: Yes

DOI: **10.22034/AJCA.2022.335594.1307**

KEYWORDS

Phytosynthesis
Nanoparticles
Olax subscorpioidea
Antimicrobial activities
Bioactive molecules

ABSTRACT

In this study, aqueous extracts of the leaf and root of *Olax subscorpioidea* were used as solvent, reducing and stabilizing agents in synthesizing silver nanoparticles (AgNPs). The change in color from colorless to dark brown indicated the AgNPs formation. The UV-Vis spectra showed active absorption at 460 nm for the root extract mediated AgNPs attributed to the surface plasmon resonance of the AgNPs. This absorbance is quite intense compared to that of the leaf, which is slightly shifted to a higher wavelength of 465 nm. The FTIR spectra showed absorption bands attributed to O-H and N-H stretching vibrations of the phenolic/amide groups. In addition, the bands due to symmetric stretching vibrations of C-H and carbonyl (C=O) groups are also observed. The bioactive molecules present in the plant extracts do stabilized not only the metal nanoparticles but also play the role of modifying the surface of the particles owing to their different functionalities. The textural properties studied using Brunauer-Emmett-Teller (BET) method gave a specific surface area of 22.84 and 39.8 m^2/g, respectively for root and leaf mediated AgNPs. Scanning electron microscopy (SEM) revealed monodisperse microspheres AgNPs, while the transmission electron microscopy (TEM) showed particles in the nanosize regime. The results of the antimicrobial activities showed the *Olax subscorpioidea* mediated-AgNPs to be effective in inhibiting the growth of bacterial strains more than the antibiotic drugs under investigation.

GRAPHICAL ABSTRACT

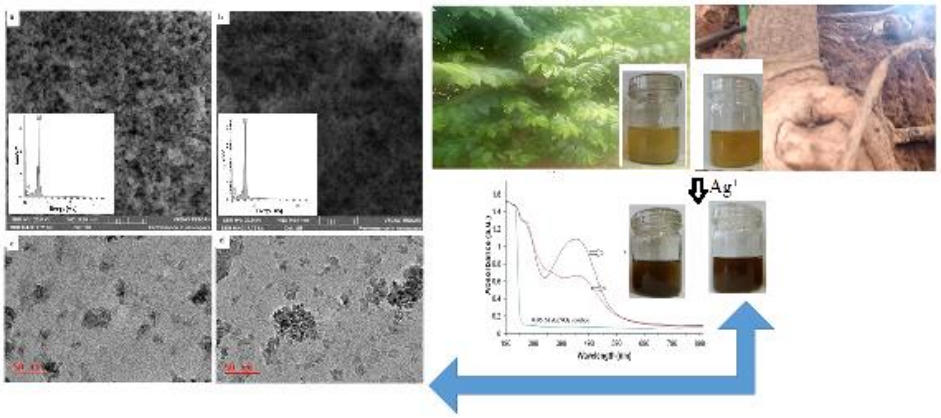

* Corresponding author: Ayi Anyama, Ayi
✉ E-mail: ayiayi72@gmail.com, a.anyama@unical.edu.ng

Introduction

Silver metal and metal nanoparticles have effectively treated bacterial and fungal infections [1-4]. Nanoparticles of silver are even more effective as an antiseptic, disinfectant, and antiviral agent. Hence, an increasing interest in the synthesis of silver nanoparticles for medical applications [2, 5-12]. Their use as microbicides is not only due to their effectiveness in small doses, low toxicity, and minimal side effects, but also for prevention of infection and antiviral therapies [5, 9].

Different protocols have been adopted to synthesize metal and metal oxide nanoparticles. One of the most common methods involves synthesis in the presence of chemical reducing agents [13-15]. The major challenge in using the chemical method ranges from the high cost of operations to a considerable amount of toxic wastes and pollutants generated at the end of the reaction. Current research interest is on the biogenic synthesis of nanoparticles involving the use of extracts from leaves, stem barks, roots, or fruits of the plant [16-22]. It has been demonstrated that nanomaterials obtained from plants extracts are economical, eco-friendly, and very stable due to the chelation of the phytochemicals [23]. Nanomaterials obtained from plant extracts are advantageous for medical applications, owing to enhanced stability via chelation by the phytochemicals, minimal off-target bindings, and neutralization of the free radicals [23, 24-27].

In our search for plants with medicinal purposes for use in the biogenic synthesis of metal nanoparticles, *Olax subscorpioidea* was chosen. *Olax subscorpioidea* is a plant that belongs to the family Olacaceae. The tree is about 10 m high, with long thin, often drooping branches (Figure 1), but sometimes a many-stemmed shrub of deciduous forest and jungles as undergrowth and thickets in savanna regions [28]. It is found in different parts of Nigeria, Zaire, Senegal, and other African countries with different names such as Ifon (Southwestern Nigeria), Mtungawezi (Swahil), Ukpakon (Edo), Aziza (South-Eastern Nigeria), and Gwano Kurmi (Northern Nigeria) [29-31]. Traditionally, *Olax subscorpioidea* plant is used as medicine to treat rheumatism, arthritis, liver disease, and venereal diseases. The root of olax subscorpioidea has effectively treated cutaneous, subcutaneous parasitic infections and as genital stimulants [28, 32-34].

Figure 1. *Olax subscorpioidea* plant a) the leaves b) the root

Because of the interesting report on the medicinal properties of *Olax subscorpioidea* and the bioactive compounds (tannins, alkaloids, flavonoids, saponins, glycosides, steroids, etc.)

responsible for its diverse biological activities, herein we report room temperature photosynthesis of silver nanoparticles using its leaf and root aqueous extracts as a solvent medium, reducing agents, and stabilizing agents. The antimicrobial activities of the *Olax subscorpioidea*-mediated silver nanoparticles have been evaluated.

Materials and Methods

Materials

All chemical reagents were of analytical grade and obtained from Merck Company, except when stated otherwise. The antibiotics were obtained over the counter from Noble Pharmaceutical Company located at number 19 Goldie Street Calabar, Cross River State, Nigeria. The fresh root and leaf of *Olax subscorpioidea* were gotten from Bayobre village in Obudu Local Government Area of Cross River State, Nigeria. Prof. David Ogar of Forestry and Wildlife and Extension, Faculty of Agriculture, University of Calabar, authenticated the plant.

Methods

Preparation of extracts

The root and leaf of *Olax subcorpioidea* were carefully washed to remove all impurities and dried under the sun for one week. These samples were placed in a freeze dryer for 72 h to remove moisture. The dried roots were ground into powder using a manual blender, and larger particles were separated with the help of a sieve. About 100 g of the root sample was soaked in 250 cm^3 deionized water using a 500 cm^3 Erlenmeyer flask. The flask was covered with foil and placed on a mechanical shaker at 80 rpm for 24 h at room temperature. To obtain the aqueous extract, homogenates were subjected to vacuum filtration using Whatman filter paper. The filtrate was concentrated using a water bath at 40 °C to a volume of 100 cm^3. The same procedure was employed for the leaf extract.

Synthesis of silver nanoparticles (AgNPs)

In a typical synthesis of silver nanoparticles (AgNPs), $AgNO_3$ (1.0 g, 5.89×10^{-2} M) was dispersed in 20 cm^3 of aqueous extract for each root and leaf of *Olax subcorpioidea* under continuous stirring using a magnetic stirrer at room temperature. Dark brown coloration of reaction mixtures (Figure 2) was observed, indicating nanoparticle formation. The products were centrifuged at 4000 rpm for 20 min, filtered and washed with distilled water, dried at room temperature, and stored in an airtight container.

Characterization of AgNPs

The active components in the extract responsible for the reduction were analyzed using FTIR Spectrophotometer (Shimadzu IR Affinity-1S) in the spectral range of 4000 to 500 cm^{-1} at 2 cm^{-1} resolution. Scanning electron microscopy (SEM) was performed on a Hitachi S-4800 microscope equipped with EDX at a voltage of 15 Kv. Transmission electron microscope (TEM) images were carried out using a JEOL-JEM-2100F electron microscope. The N_2 sorption measurements were performed on a Micromeritics ASAP 2460 sorption system using the Brunauer-Emmett-Teller (BET) method.

Antimicrobial assays

An antimicrobial susceptibility test was carried out in the bacteriology lab of the General Hospital Calabar, Cross River State, Nigeria.

Antibacterial assay

Different concentrations of aqueous extracts of plant root and leaf AgNPs were tested for bioactivity against *Staphylococcus aureus* (ATCC 43200), *Enterococcus faecalis* (ATCC 5130), *Escherichia coli* (ATCC 35218), *Pseudomonas*

aeruginosa (ATCC 27852) and *Klebsiella pneumoniae* (ATCC 700602). The broth microdilution method was employed to determine the minimum inhibitory concentration (MIC). Serial two-fold concentrations of AgNPs and root and leaf tissue were prepared in sterile 96-well plates over 200-1.25 g/dm^3. The first row (name row 1) of the plates was reserved for blank/negative and uninhibited growth controls, and these wells were filled with Mueller Hinton (MH) media only. Wells were then inoculated with diluted overnight broth culture initially adjusted to 0.5 McFarland turbidity standard gives the optical density when compared to the density of bacterial suspension colony forming the units and incubated at room temperature for 15-24 h. Subsequently, 40 dm^3 of freshly prepared iodonitrotetrazolium chloride (INT) was added to all wells, and the plates were incubated in the dark for 18 h at room temperature. The INT reagent, initially colorless, was reduced to a red product following incubation. This reduction resulted from continued bacterial growth, while no color change denoted the inhibition or lack of bacterial growth. The absorbance was determined at 630 nm using a multi-model plate reader (Biotek Synergy HT, USA) with Gen 5 software. Neomycin served as a positive control. The MIC was defined as the lowest concentration of an antimicrobial agent that inhibits the growth of a microorganism after overnight incubation. The exact process was done for the leaf extracts.

Antifungal assay

The exact concentration range was used to determine the antifungal activity of AgNPs root and leaf material according to the broth microdilution method as prescribed by the NCCLS guidelines. The plates were prepared as described in the antibacterial assay, except that saboraud 2% dextrose (SD) broth was used instead of MH broth. Three candida reference strains, *Candida albicans* (ATCC 90027), *Candida krusei* (ATCC 6257), and *Candida parapsilosis* (ATCC 22018) were inoculated into a freshly prepared SD broth and grown aerobically overnight at room temperature in an Infor's HT multritron environmental shaker at 100 rpm. Cells were harvested by centrifugation and resuspended in 1% saline after that. The absorbance of resuspended starter cultures was determined spectrophotometrically. To conform to McFarland's standards, the cells were diluted using SD broth to achieve optical densities in 0.08-0.10. As soon as this was achieved, the working suspension was diluted (1:20) in RPMI 1640 medium with L-glutamine, without bicarbonate and phenol red. (Biochrom Berlin). The working suspension was further diluted (1:50) with RPMI 1640 to obtain the final test inoculum concentration of 1-5 x 10^3 CFU mL^{-1}. Aliquots (100 cm^3) of inoculum were added to all wells of the test microtiter plates except the blank/negative control wells. The plates were incubated aerobically at room temperature for 24 h. After incubation, 20 dm^3 of 3-(4,5-dimethylthiazol-2-yl)-2-5-(3-carboxy-methoxyphenyl)-2-(4-sulfophenyl)-2H tetrazolium salt was added to all wells and incubated in the dark at room temperature for 24 h. The absorbance was determined at 490 cm^3. The commercially available antibiotic amphotericin B was used as a positive control. All the experiments were carried out in triplicate.

Results and Discussion

The phytochemical screenings of aqueous extract of the leaves, stem barks, and root of *Olax subcorpioidea* revealed the presence of tannins, flavonoids, terpenoids, steroids, alkaloids, saponins, phenols, and carotenoids [22, 32]. In this study, aqueous extracts of the leaves and roots were used as a solvent, reducing and stabilizing agents in synthesizing silver nanoparticles. In a typical synthesis using the

root extracts, 20 cm^3 of root extracts of *O. subcorpoidea* was added to 0.05 M $AgNO_3$ solution under constant stirring at room temperature. The change in color from colorless to dark brown, as shown in Figure 2 indicated the formation of silver nanoparticles (AgNPs). In Figure 3, the UV-vis analyses of the particles are presented. The UV-Vis spectra showed active absorption at 460 nm for the root extract mediated AgNPs attributed to the surface plasmon resonance of the AgNPs. This absorbance is quite intense compared to that of the leaf, which is slightly shifted to a higher wavelength of 465 nm.

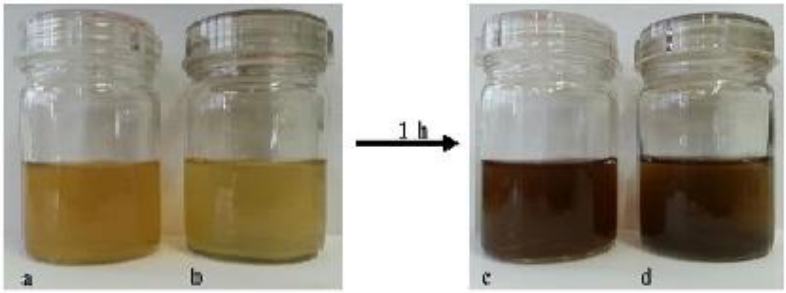

Figure 2. (a) Aqueous root extract of *Olax subcorpioidea* (b) aqueous leaf extract of *Olax subcorpioidea* (c) root extract mediated AgNPs (d) leaf extract mediated AgNPs

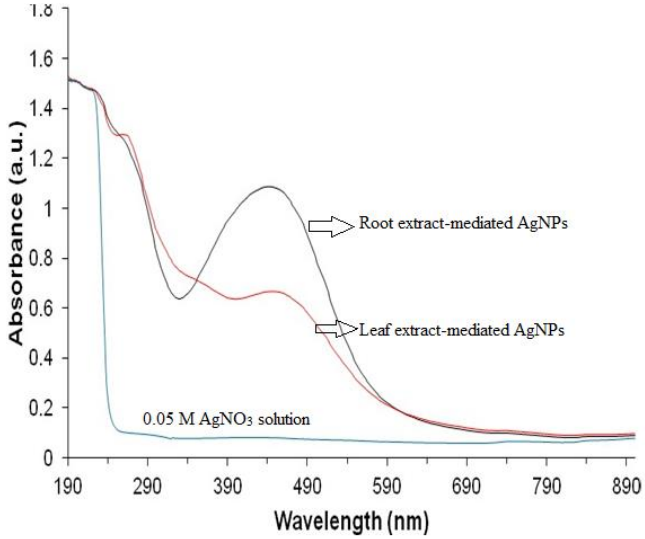

Figure 3. UV-visible spectra of the *Olax subcorpioidea*-mediated AgNPs

The FTIR spectra of the aqueous root and leaf extracts (Figures 4a and b) and their respective AgNPs (Figures 4c and d) revealed the presence of biomolecules responsible for the reduction and efficient stabilization of the silver nanoparticle synthesized by *Olax subscorpioidea*. The absorption bands at 3272 cm^{-1} and 3271 cm^{-1} for the root and leaf extracts, respectively, are attributed to the O-H and/or N-H stretching vibrations of the phenolic/amide groups. These bands shifted downward to 3033 and 3199 cm^{-1} for root and leaf-mediated AgNPs, respectively. The bands at 2919 and 2850 (root extract), shifted to 2947 cm^{-1} in the obtained AgNPs, and

2920 cm^{-1} (leaf extract), shifted to 2917 cm^{-1} in the leaf-mediated AgNPs, are due to symmetric stretching vibrations of C-H groups. The absorption vibrational bands at the region 1626-1454 cm^{-1} (root extract), 1626, 1513 cm^{-1} (root-mediated AgNPs) and 1624-1531 cm^{-1} (leaf extract), 1629-1513 cm^{-1} (leaf-mediated AgNPs) can be attributed to carbonyl (C=O) groups. The vibration of the C-N group of the amide/amine observed at 1233 (root), and 1392 cm^{-1} (leaf extract) shifted to 1380 cm^{-1} in the plant-mediated AgNPs. The vibrations of the C=C groups of the aromatic rings are observed at 1403 (root) and 1449 cm^{-1} (leaf extract). The stretching vibrational modes of O-C-O groups are observed at 1032 and 1070 cm^{-1}, respectively, for the root and leaf extracts. The bands observed at 526 cm^{-1} (root extract) and 532 cm^{-1} (leaf extract) shift slightly to a lower frequency of 495, and 517 cm^{-1} for AgNPs obtained from root and leaf extracts, respectively. These bands can be attributed to either the peptide linkages' N-H bending modes or the acid halides' C-X bonds. The various assignments agree with literature reports for similar compounds [15, 21-23].

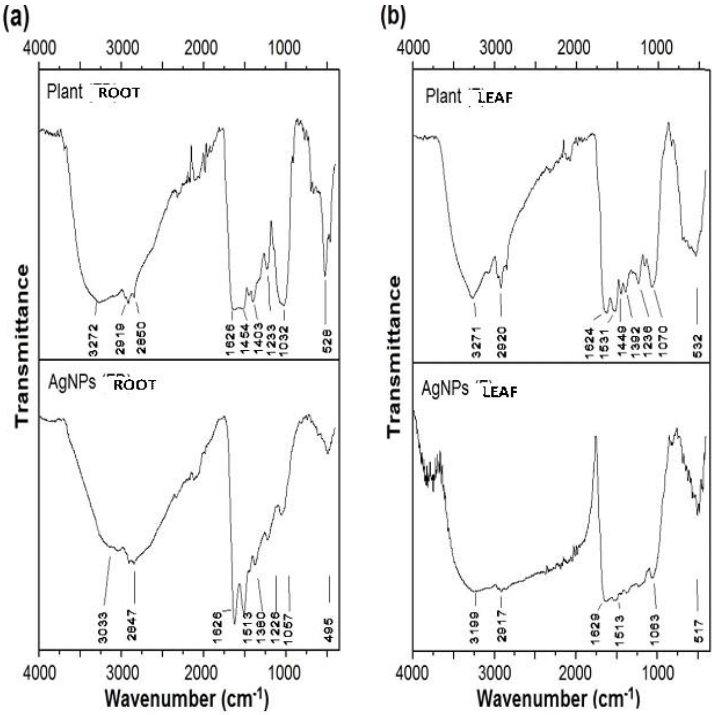

Figure 4. FTIR spectra of the aqueous extracts of *Olax subcorpioidea* and the synthesized AgNPs

The phytochemicals present in the extracts form a protective layer around the silver nanoparticles, thereby stabilizing them in a core-shell mode [12, 35]. The reactive groups not only stabilize the metal nanoparticles but also play the role of surface modification of the particles. To evaluate the pore structure properties of the surface-modified AgNPs, nitrogen adsorption-desorption measurement was performed on the as-synthesized particles using the BET method. The N_2 adsorption-desorption isotherm of the silver nanoparticles is presented in Figure 5. The BET analysis gave a specific surface area of 22.84 m^2/g, pore volume of 20.07 cm^3/g, and pore size of 13.7 nm for the root extract-mediated AgNPs, while that of leaf extract was found to have a specific surface area of 39.8 m^2/g, pore volume of 20.12 cm^3/g and pore size of 12.95 nm. The isotherm is mainly a type III, indicating unrestricted multilayers formation process. This

is because the interactions between the adsorbed molecules (adsorbate-adsorbate interactions) are strong compared with adsorbent surface-adsorbate interactions [36].

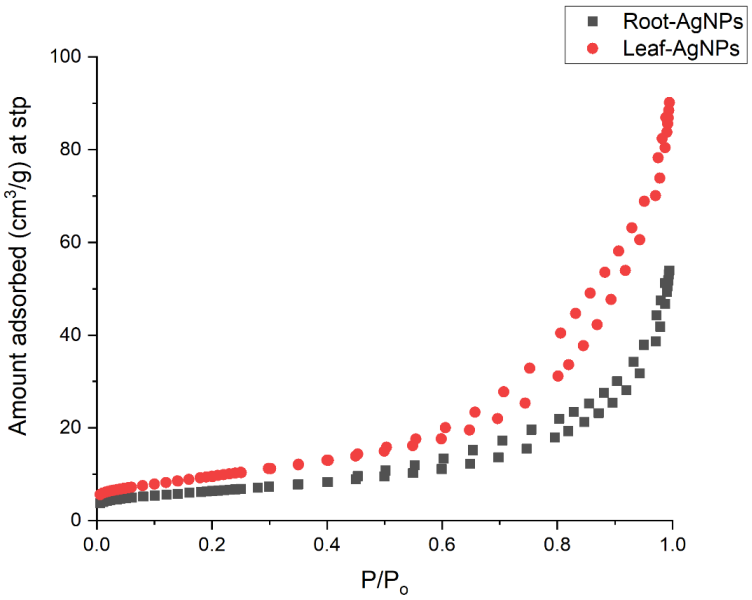

Figure 5. N_2 adsorption-desorption isotherm of Olax subcorpioidea mediated AgNPs

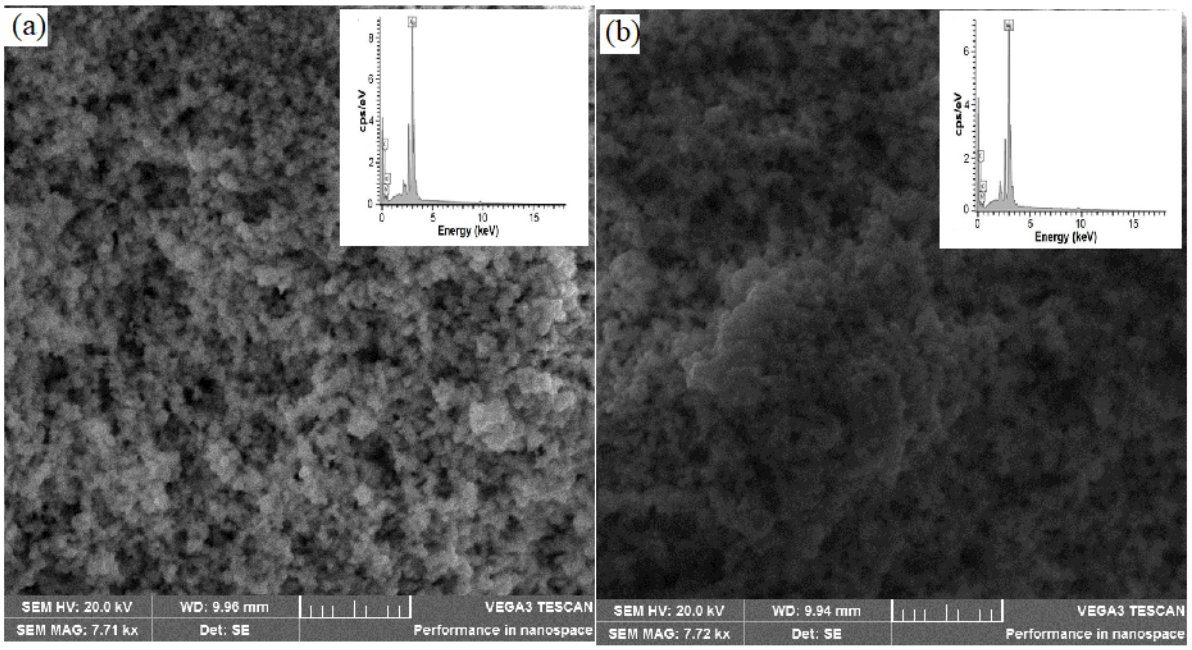

Figure 6. Representative SEM images of (a) AgNPs obtained from the aqueous root extract of *Olax subscorpioidea* and (b) AgNPs obtained from aqueous leaf extract of *Olax subscorpioidea*. Insert: Energy Dispersive Analyses by X-ray (EDX)

The representative scanning electron (SEM) and transmission electron (TEM) images of the AgNPs synthesized using aqueous extracts of *Olax subscorpioidea* are respectively shown in

Figures 6 and 7. The SEM revealed monodisperse microspheres AgNPs. The energy dispersive

X-ray (EDX) overall scans of both the root (inset of Figure 6a) and leaf (inset of Figure 6b) mediated AgNPs showed peaks between 0–1 k eV, indicating the presence of carbon, nitrogen, and oxygen originating from the secondary metabolites in the plant extracts, which acts as stabilizers. The intense and robust peak around 3.0 keV corresponds to the binding energies of AgNPs. These peaks agree with a similar report in the literature [15]. The representative TEM micrographs of the AgNPs obtained from both root and leaf extracts showed an average size of 50 nm.

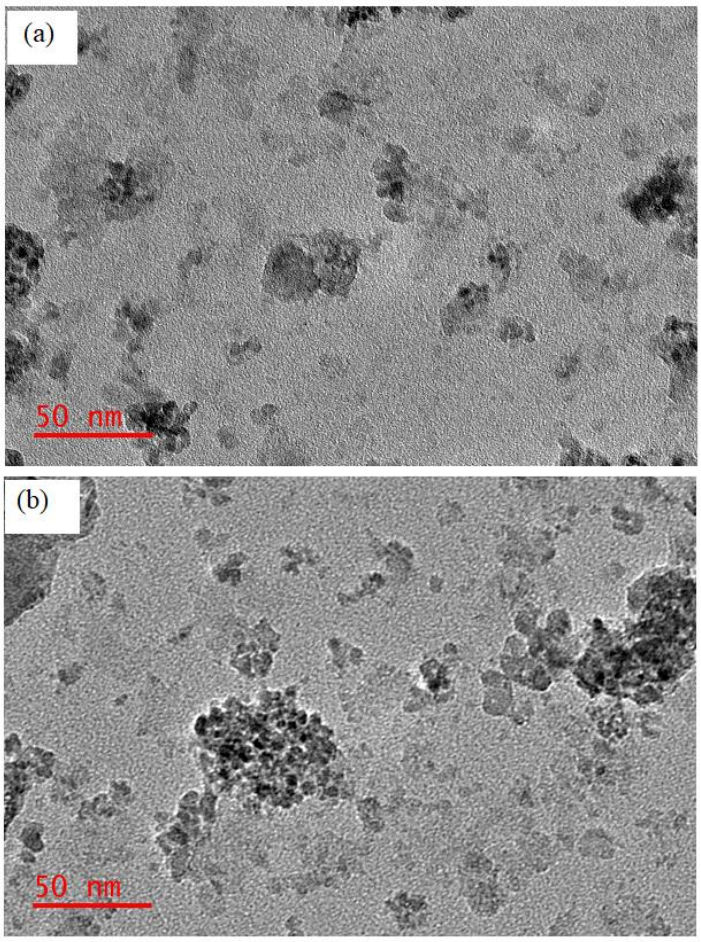

Figure 7. Representative TEM images of (a) root extract of *Olax subscorpioidea* mediated AgNPs and (b) leaf extract of *Olax subscorpioidea* mediated AgNPs

The antimicrobial activities of the synthesized AgNPs were evaluated using a standard assay. The antimicrobial activities of aqueous extracts of both the root and leaf of Olax subscorpioidea mediated-AgNPs are presented in Table 1. Neomycin, an over-the-counter antibiotic, was used to control bacterial strains, while amphotericin B served as control for the fungal strains. The results showed AgNPs (30 mg/cm^3) to inhibit the growth of five bacterial strains (*E. coli*, *E. feacalis*, *K. pneumonia*, *P. aeruginosa*, *and S. aureus*) and reasonable inhibition for the fungal strains. The representative plates showing the zones of inhibition are presented in Figure 8. The Zone of Inhibition (ZOI) for *E. coli* and *E. feacalis* was 12.5 mm for both roots and leaf

extracts and the mediated AgNPs. The ZOI for *K. pneumonia*, *P. aeruginosa* and *S. aureus* were 25.0 mm. The control drug, neomycin, did not affect *E. feacalis*, *P. aeruginosa,* and *S. aureus*, but inhibited *K. pneumonia*, (ZOI=25.0 mm) and E. coli (ZOI=6.25 mm).

Table 1. Antimicrobial activities of aqueous extracts of Olax subscorpioidea mediated AgNPs

Microorganisms	Root-AgNPs	Leaf-AgNPs	Neomycin
Bacterial strains			
E. coli	12.5±0.01	12.5±0.01	6.25±0.04
E. faecalis	12.5±0.01	12.5±0.00	-
K. pneumoniae	25±0.01	25±0.02	25±0.04
P. aeruginosa	25±0.01	25±0.01	-
S. aureus	25±0.03	25±0.04	-
Fungal strains			**Amphotericin B**
C. Krusei	6.25±0.02	6.25±0.02	0.02±0.00
C. albicans	6.25±0.03	6.25±0.02	0.02±0.00
C. parapsilosis	6.25±0.02	6.25±0.01	0.02±0.00

Figure 8. Representative plates showing antimicrobial activities of aqueous extracts the root and leaf of Olax subscorpioidea mediated AgNPs

Conclusion

Aqueous root and leaf extracts of *Olax subscorpioidea* have been successfully used to synthesize silver nanoparticles at room temperature. The aqueous extracts, which are non-toxic and eco-friendly, served as a solvent medium, reducing and stabilizing agents. The secondary metabolites present in the plant extracts stabilized the metal nanoparticles. They played the role of surface modification of the particles giving BET specific surface area of 22.84 and 39.8 m^2/g, respectively, for root and leaf mediated AgNPs. The surface plasmon resonance for the AgNps was observed at 430-460 nm. The *Olax subscorpioidea* mediated-AgNPs have shown effectiveness against the growth of bacterial and fungal strains investigated in this study. However, further studies should be carried out to investigate the effect of temperature on the stability of the plant-mediated AgNPs and their antioxidant properties.

Acknowledgment

The authors thank Dr. Charles Ojiefoh Oseghale, Department of Chemistry, University of Johannesburg, Auckland Park, South Africa for help with BET, SEM and TEM analyses.

Disclosure statement

The authors reported no potential conflict of interest.

ORCID

Ayi Anyama Ayi: 0000-0002-4908-9929

References

[1] J.S. Kim, E. Kuk, K.N. Yu, J.H. Kim, S.J. Park, H.J. Lee, S.H. Kim, Y.K. Park, Y.H. Park, C.Y. Hwang, Y.K. Kim, Y.S. Lee, D.H. Jeong, M.H. Cho, *Nanomedicine*, **2007**, *3*, 95–101. [CrossRef], [Google Scholar], [Publisher]

[2] H.H. Lara, N.V. Ayala-Nuñez, L. Ixtepan-Turrent, C. Rodriguez-Padilla, *World J. Microbiol. Biotechnol.*, **2010**, *26*, 615–621. [CrossRef], [Google Scholar], [Publisher]

[3] O.V. Salata, *J. Nanobiotechnology*, **2004**, *2*, 3. [CrossRef], [Google Scholar], [Publisher]

[4] A.R. Shahverdi, A. Fakhimi, H.R. Shahverdi, S. Minaian, *Nanomedicine*, **2007**, *3*, 168–171. [CrossRef], [Google Scholar], [Publisher]

[5] H.H. Lara, N.V. Ayala-Nuñez, L. Ixtepan-Turrent, C. Rodriguez-Padilla, *J. Nanobiotechnology*, **2010**, *8*, 1. [CrossRef], [Google Scholar], [Publisher]

[6] J.R. Furr, A.D. Russell, T.D. Turner, A. Andrews, *J. Hosp. Infect.*, **1994**, *27*, 201–208. [CrossRef], [Google Scholar], [Publisher]

[7] I. Sondi, B. Salopek-Sondi, *J. Colloid Interface Sci.*, **2004**, *275*, 177–182. [CrossRef], [Google Scholar], [Publisher]

[8] M. Gajbhiye, J. Kesharwani, A. Ingle, A. Gade, M. Rai, *Nanomedicine*, **2009**, *5*, 382–386. [CrossRef], [Google Scholar], [Publisher]

[9] H.H. Lara, L. Ixtepan-Turrent, E.N. Garza-Trevino, C. Rodriguez-Padilla, *J. Nanobiotechnology*, **2010**, *8*, 15. [CrossRef], [Google Scholar], [Publisher]

[10] C. Baker, A. Pradhan, L. Pakstis, D.J. Pochan, S. Shah, *J. Nanosci. Nanotechnol.*, **2005**, *5*, 244–249. [CrossRef], [Google Scholar], [Publisher]

[11] M. Rai, A. Yadav, A. Gade, *Biotechnol. Adv.*, **2009**, *27*, 76–83. [CrossRef], [Google Scholar], [Publisher]

[12] A.A. Ayi, C.A. Anyama, V. Khare, *J. Mater.*, **2015**, *2015*, 1–7. [CrossRef], [Google Scholar], [Publisher]

[13] W.E. John, A.A. Ayi, C.A. Anyama, P.B. Ashishie, B.E. Inah, *Adv. J. Chem. A*, **2019**, *2*, 175–183. [CrossRef], [Google Scholar], [Publisher]

[14] A.A. Ayi, V. Khare, P. Strauch, J. Girard, K.M. Fromm, A. Taubert, *Monatsh. Chem.*, **2010**, *141*, 1273–1278. [CrossRef], [Google Scholar], [Publisher]

[15] P.B. Ashishie, C.A. Anyama, A.A. Ayi, C.O. Oseghale, E.T. Adesuji, A.H. Labulo, *Int. J. Phys. Sci.*, **2018**, *13*, 24–32. [CrossRef], [Google Scholar], [Publisher]

[16] M. Satish Kumar, K. Sneha, S.W. Won, C.W. Cho, S. Kim, Y.S. Yun, *Colloids Surf. A*, **2009**, *73*, 332–338. [CrossRef], [Google Scholar], [Publisher]

[17] S.K. Sivarraman, I. Elango, S. Kumar, V. Santhanam, *Curr. Sci.*, **2009**, *97*, 1055–1059. [Google Scholar], [Publisher]

[18] A. Tripathi, N. Chandrasekaran, A.M. Raichur, A. Mukherjee, *J. Biomed. Nanotechnol.*, **2009**, *5*, 93–98. [CrossRef], [Google Scholar], [Publisher]

[19] T.C. Prathna, N. Chandrasekaran, A.M. Raichur, A. Mukherjee, *Colloids Surf. B*, **2011**, *82*, 152–159. [CrossRef], [Google Scholar], [Publisher]

[20] A. Mubayi, S. Chatterji, P.M. Rai, G. Watal, *Adv. Mat. Lett.*, **2012**, *3*, 519–525. [CrossRef], [Google Scholar]

[21] P.P.N. Vijaykumar, S.V.N. Pammi, P. Kollu, K.V.V. Satyanarayana, U. Shameem, *Ind. Crops Prod*., **2014**, *52*, 562–566. [CrossRef], [Google Scholar], [Publisher]

[22] I.C. Orabueze, A.A. Amudalat, A.A. Usman, *J. Pharmacogn. Phytochem.*, **2016**, *5*, 398–406. [Google Scholar], [Publisher]

[23] M. Riaz, A. Suleman, P. Ahmad, M.U. Khandaker, A. Alsqahtanin, D.A. Bradley, M.Q. Khan, *Crystals*, **2022**, *12*, 252. [CrossRef], [Google Scholar], [Publisher]

[24] S. Ahmad, S. Munir, N. Zeb, A. Ullah, B. Khan, J. Ali, M. Balal, M. Omer, M. Alamzeb, S.M. Salman, S. Ali, *Int. J. Nanomol*., **2019**, 5087–5107. [CrossRef], [Google Scholar], [Publisher]

[25] N. Gupta, A.R.H Fischer, L.J. Frewer, *NanoEthics*, **2015**, *9*, 93–108. [CrossRef], [Google Scholar], [Publisher]

[26] H.K. Kehri, I. Zoomi, U. Singh, D. Pandey, *J. Nanosci. Technol*., **2019**, *5*, 810–816. [Google Scholar]

[27] V.V. Makarov, A.J. Love, O.V. Sinistsyna, S.S. Makarova, I.V. Yaminsky, M.E. Taliansky, N.O. Kalinina, *Acta Nat*., **2014**, *6*, 35–44. [Google Scholar], [Publisher]

[28] E. Adegoke, A. Akinsanya, A. Nagu, *J. West Afric. Sci. Ass*., **1968**, *13*, 13–39. [Google Scholar]

[29] A.A. Ayandele, A.O. Adebiyi, *Afr. J. Biotechnol*., **2007**, *6*, 868–870. [Google Scholar], [Publisher]

[30] A.H. Adebayo, O.S. Adegbite, J.O. Olugbuyiro, O.O. Famodu, K.B. Odenigbo, *Afri. J. Pharm. Pharmocol.*, **2014**, *8*, 570–578. [Google Scholar]

[31] C.V. Ukwe, C.M. Ubaka, U.J. Madusque, *Asian Pac. J. Trop. Med.,* **2010**, *3*, 13–16. [CrossRef], [Google Scholar], [Publisher]

[32] N.N. Ezeani, U.A. Ibiam, I.O. Orji, E.U. Alum, P.M. Aja, I.O. Igwenyi, P.C. Ugwu, C. Aloke, *J. Pharm. Chem. Pharmocol.*, **2018**, *2*, 1–11. [CrossRef], [Google Scholar], [Publisher]

[33] I.K. Mutiu, O.A. Ademola, M. Emmanuel, *Int. J. Pharmarmcol.*, **2015**, *11*, 484–489. [CrossRef], [Google Scholar], [Publisher]

[34] K. Konan, B.L.N.K. Justin, M. Souleymane, Y.A. Francis, *Pharmacogn. Mag*., **2015**, *11*, 111–116. [CrossRef], [Google Scholar], [Publisher]

[35] E.J.W. Verwey, J.T.G. Overbeek, *Theory of the Stability of Lyophobic Colloids*, Dover Publications, Mineola, NY, USA, 2nd edition, **1999**. [Google Scholar]

[36] M. Thommes, K. Kaneko, A.V. Neimark, J.P. Olivier, F. Rodrigues-Reinoso, J. Rouquerol, K.S. W. Sing, *Pure Appl. Chem*., **2015**, *87*, 1051–1069. [CrossRef], [Google Scholar], [Publisher]

HOW TO CITE THIS ARTICLE

Ochui Isaac Ashindortiang, Chinyere Ayi Anyama, Ayi Anyama Ayi*. Phytosynthesis, Characterization and Antimicrobial Studies of Silver Nanoparticles Using Aqueous Extracts of *Olax Subscorpioidea*. *Adv. J. Chem. A*, **2022**, 5(3), 215-225.

DOI: 10.22034/AJCA.2022.335594.1307
URL: http://www.ajchem-a.com/article_149182.html